**Atmospheric
Chemistry
and Physics**

Trends of HCl, ClONO$_2$, and HF column abundances from ground-based FTIR measurements in Kiruna (Sweden) in comparison with KASIMA model calculations

R. Kohlhepp[1], S. Barthlott[1], T. Blumenstock[1], F. Hase[1], I. Kaiser[1], U. Raffalski[2], and R. Ruhnke[1]

[1]Karlsruhe Institute of Technology (KIT), Institute for Meteorology and Climate Research (IMK), Karlsruhe, Germany
[2]Swedish Institute of Space Physics (IRF), Kiruna, Sweden

Abstract. Trends of hydrogen chloride (HCl), chlorine nitrate (ClONO$_2$), and hydrogen fluoride (HF) total column abundances above Kiruna (Northern Sweden, 67.84° N, 20.41° E) derived from nearly 14 years (1996–2009) of measurement and model data are presented. The measurements have been performed with a Bruker 120 HR (later Bruker 125 HR) Fourier transform infrared (FTIR) spectrometer and the chemistry-transport model (CTM) used was KASIMA (KArlsruhe SImulation model of the Middle Atmosphere). The total column abundances of ClONO$_2$ and HF calculated by KASIMA agree quite well with the FTIR measurements while KASIMA tends to underestimate the HCl columns.

To calculate the long-term trends, a linear function combined with an annual cycle was fitted to the data using a least squares method. The precision of the resulting trends was estimated with the bootstrap resampling method.

For HF, both model and measurements show a positive trend that seems to decrease in the last few years. This suggests a stabilisation of the HF total column abundance. Between 1996 and 2009, KASIMA simulates an increase of $(+1.51\pm0.07)$ %/yr which exceeds the FTIR result of $(+0.65\pm0.25)$ %/yr.

The trends determined for HCl and ClONO$_2$ are significantly negative over the time period considered here. This is expected because the emission of their precursors (chlorofluorocarbons and hydrochlorofluorocarbons) has been restricted in the Montreal Protocol in 1987 and its amendments and adjustments. The trend for ClONO$_2$ from the FTIR measurements amounts to (-3.28 ± 0.56) %/yr and the one for HCl to (-0.81 ± 0.23) %/yr. KASIMA simulates a weaker decrease: For ClONO$_2$, the result is (-0.90 ± 0.10) %/yr and for HCl (-0.17 ± 0.06) %/yr. Part of the difference between measurement and model data can be explained by sampling and the stronger annual cycle indicated by the measurements. There is a factor of about four between the trends of HCl and ClONO$_2$ above Kiruna for both measurement and model data.

1 Introduction

Since the 1970s, anthropogenic chlorofluorocarbons (CFCs), hydrochlorofluorocarbons (HCFCs), and halons have been predicted to deplete the stratospheric ozone layer (Molina and Rowland, 1974). A few years afterwards, measurements showed a strong decrease of ozone column abundances above Antarctica in the Southern Hemisphere spring which was then called the Antarctic ozone hole. As a result of this discovery, the emission of CFCs and HCFCs was restricted in the Montreal Protocol in 1987 and its amendments and adjustments.

Since then, stratospheric ozone has been monitored closely by many different measurement techniques. In addition, it is very important to know the concentration of the ozone-depleting substances to be able to check the effectiveness of the Montreal Protocol and to predict the development of the ozone layer.

From the atmospheric content of the chlorine reservoir gases hydrogen chloride (HCl) and chlorine nitrate (ClONO$_2$), it is possible to infer the amount of activated chlorine which is able to deplete ozone. Together, HCl and ClONO$_2$ represent about 90 % of all inorganic chlorine in the stratosphere.

Hydrogen fluoride (HF) in the middle atmosphere results nearly exclusively from the photo-dissociation of anthropogenic CFCs and HCFCs and thus is a valuable indicator for man-made changes. The stratospheric lifetime of HF is more than ten years so that it can be treated as an inert tracer there (see also Chipperfield et al., 1997). As fluorine does not play an important role in stratospheric ozone depletion, there are no direct restrictions concerning its emission like the Montreal Protocol for chlorine and bromine, for example. But it is also contained in CFCs and HCFCs, so it is expected to be influenced by the Montreal Protocol, too.

In this paper, measurements of vertical columns of HCl, ClONO$_2$, and HF with a Fourier transform infrared (FTIR) spectrometer at Kiruna (Northern Sweden, 67.84° N, 20.41° E, 419 m a.s.l.) are presented. They are compared with results from the atmospheric chemistry transport model (CTM) KASIMA (KArlsruhe SImulation model of the Middle Atmosphere) and also with the longest European FTIR time series recorded on Jungfraujoch (Swiss Alps, 46.5° N, 8.0° E, 3580 m a.s.l.) (see e.g. Zander et al., 2008). The key question addressed is whether the expected decrease of chlorine species can already be seen significantly in the vertical column abundances of HCl and ClONO$_2$ above Kiruna and how the HF abundances develop.

In Sects. 2 and 3, the FTIR data acquisition and the KASIMA model, respectively, are described. Section 4 explains the bootstrap method used to estimate the precision of the calculated trends. The results are presented in Sect. 5 and summarised in Sect. 6.

2   FTIR data

Within the "Network for the Detection of Atmospheric Composition Change (NDACC)", measurements with a Fourier transform infrared spectrometer are performed in Kiruna in a cooperation between the Swedish Institute of Space Physics (IRF) in Kiruna, Sweden, the University of Nagoya, Japan, and the Institute for Meteorology and Climate Research (IMK-ASF) at the Karlsruhe Institute of Technology (KIT), Germany. The measurements at this site were started in March 1996. For the analysis here, results until November 2009 were included so that the time series are about 14 years long.

The instrument used first was a Bruker 120 HR Fourier transform spectrometer (FTS) which was upgraded to a 125 HR in July 2007. This upgrade only consisted in a change of the electronics and the scanner motor. Since the beginning of the measurements, the spectrometer is regularly quality-controlled by cell measurements as described by Hase et al. (1999). Within the error bar of the cell measurement (a few percent), the instrumental line shape (ILS) is equivalent to the theoretical one.

In winter, Kiruna is usually influenced by the stratospheric polar vortex so that atmospheric polar processes can be investigated with the spectrometer. As Kiruna is close to the Arctic circle, the polar night is quite short (about 1.5 months). This is a very important aspect because for the kind of measurements analysed here, the FTIR instrument needs the sun as the source of radiation.

From the obtained spectra, column abundances (and vertical profiles) of various atmospheric trace gases absorbing in the infrared spectral region are determined with the inversion code PROFFIT (Hase, 2000; Hase et al., 2004). To calculate the a priori spectra needed for the inversion process, PROFFIT uses daily temperature and pressure profiles for Kiruna from NCEP (National Centers for Environmental Prediction) analyses provided by the automailer system of NASA's Goddard Space Flight Center. The required spectroscopic line data was taken from the HITRAN (HIgh-resolution TRANsmission molecular absorption) 2004 database (Rothman et al., 2005). The ClONO$_2$ cross sections in this dataset were provided by Wagner and Birk (2003). For HCl and HF, a Galatry lineshape function was used (Barret et al., 2005).

The time series analysed here consist of daily mean column abundances. The HCl series contains 978 data points for the whole time period (about 14 years), the ClONO$_2$ one 1004 and the HF series 915. The numbers differ slightly because not every spectral filter region can be measured every day, for example due to changes in the weather.

For each of the three investigated species, the height-dependent sensitivity of the retrieval was calculated for every measured spectrum on the 45 levels used, between 0 and 85 km. Example curves for the sensitivity are shown in Fig. 1. They are mean values, each one calculated from six arbitrary spectra with different solar elevation angles. The sensitivity shown here is defined as the sum of the columns of the averaging kernel matrix. That means the elements of the averaging kernels were summed up for every height level as described by Vigouroux et al. (2008). This sensitivity is quite good in the stratosphere (about 15 to 50 km) as the values are nearly equal to 1, while in the troposphere, it is much smaller, especially for ClONO$_2$. The HCl measurement has about 3.1 degrees of freedom for signal (DOFS) which means the vertical resolution amounts to roughly 10 km (from the ground up to about 35 km), and for HF, 2.5 DOFS can be obtained, corresponding to about 10 km vertical resolution, too (from the ground up to about 30 km). From ClONO$_2$, only the vertical column can be determined as it has only about 1.1 DOFS.

The mean relative statistical error amounts to around 29 % for ClONO$_2$, 1.2 % for HCl, and 1.5 % for HF (calculated after Rodgers, 2000). The ClONO$_2$ random error is much larger than those of HF and HCl because ClONO$_2$ is more difficult to retrieve from the measurements due to its weak spectral signature and the relatively low total column abundances especially in summer.
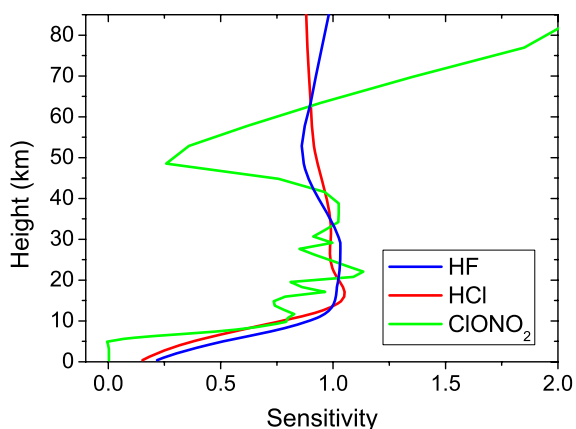
Fig. 1. Height dependency of the sensitivity of the retrieval as defined by Vigouroux et al. (2008) for HF (blue line), HCl (red line), and ClONO$_2$ (green line). This total column sensitivity describes the change in the retrieved total column, Δcol$_{retr}$, which results from a partial column change Δcol$_{inp}(h)$ applied at altitude h. The resulting sensitivity is given by sens$(h) = \Delta$col$_{retr}/\Delta$col$_{inp}(h)$. The curves shown represent mean values each calculated from six arbitrary spectra with different solar elevation angles ranging from about 2 to 38°.

3 KASIMA model data

The 3-D chemistry transport model KASIMA used in this study is a global circulation model including stratospheric chemistry for the simulation of the behaviour of physical and chemical processes in the middle atmosphere (Kouker et al., 1999; Reddmann et al., 2001; Ruhnke et al., 1999). The meteorological component is based on a spectral architecture with the pressure altitude $z = -H\ln(p/p_0)$ as vertical coordinate where $H = 7$ km is a constant atmospheric scale height, p is the pressure, and $p_0 = 1013.25$ hPa is a constant reference pressure.

For the present study, the KASIMA version as described in Reddmann et al. (2001) which yields realistic stratospheric age of air values (Stiller et al., 2008) is applied. The necessary meteorological data of temperature, vorticity and divergence are taken from the European Centre for Medium-Range Weather Forecasts (ECMWF), using ERA-40 data until 2002 and operational ECMWF analyses from 2003 on. In this version, the KASIMA model is relaxed (nudged) toward the ECMWF data between 18 and 48 km pressure altitude using forcing terms with a timescale of 4 h. Below 18 km, the meteorology is based on ECMWF analyses without nudging, and above 48 km pressure altitude, the prognostic model integrating the primitive equations without additional forcing from ECMWF data is used. The model consists of 63 vertical layers between 7 and 120 km and has a horizontal resolution of approximately 5.6° × 5.6° (T21).

The time evolution of the global surface volume mixing ratios of the ozone-depleting substances is prescribed at the lower model boundary according to the baseline scenario Ab which is a best-guess scenario following the Beijing Amendments in 1999 of the Montreal protocol (for more information on the scenario see chapter 1 of WMO, 2003). These data which were recommended to be used as lower boundary conditions for the WMO Ozone assessment 2007 are provided in the framework of the SPARC (Stratospheric Processes And their Role in Climate Change) CCM-Val (Chemistry-Climate Model Validation activity) initiative.

The photolysis rates are calculated online in KASIMA using the Fast-J2 model of Bian and Prather (2002).

For the comparison of the KASIMA model data with the FTIR measurements, the model data were interpolated to the location of Kiruna from the circumjacent grid points.

4 Trend analysis method

Largely due to Kiruna's high northern latitude, the column abundances of the investigated gases exhibit a non-negligible annual cycle. To account for this, a third order Fourier series is included in the fitting function as follows:

$$f(t) = p_1(1 + p_2 t)A(t) \qquad (1)$$

with

$$A(t) = \left(1 + \sum_{i=1}^{3} q_i \cos(2i\pi t) + r_i \sin(2i\pi t)\right) \qquad (2)$$

where t is the time in years relative to 1 January 2000 (12:00 UTC). In total, eight fitting parameters are used: p_1, p_2, q_i, and r_i ($i = 1, 3$). From the linear part of the fitting function, $p_1(1 + p_2 t)$, the increase or decrease with time is determined, while the periodic part, $A(t)$, represents the seasonal cycle. Because the absolute total column abundances of KASIMA and FTIR measurements differ especially for HCl, the trend results in this paper are not only given in absolute values (i.e. in units molec/(cm^2 yr)), but also normalised by a representative total column amount in order to enable a better comparison of the results. For this normalisation, the value of the linear part of the fit at $t = 0$ (i.e. on 1 January 2000, 12:00 UTC) is used, corresponding to p_1. As $p_1 p_2$ represents the trend in molec/(cm^2 yr), the normalised (from now on called "relative") trend corresponds to the parameter p_2, given in %/yr here.

When calculating trends of stratospheric and tropospheric trace gases from measurements by FTIR instruments, Gardiner et al. (2008) found that a third order Fourier series was the best balance between representing the time series and avoid over-fitting the data.

A least squares method is used to fit the function in Eq. (1) to the data.

Table 1. Absolute and relative trends for HF column abundances from the FTIR measurements and KASIMA model calculations for Kiruna. The time range considered is 1996–2009 unless otherwise identified. The "summer/autumn" time series contain the data between June and November only.

data source	relative trend (%/yr)	absolute trend (10^{13} molec/(cm² yr))
FTIR	+0.65±0.25	+1.32±0.50
FTIR summer/autumn	+1.10±0.23	+2.02±0.40
FTIR 1996–2002	+0.65±0.69	+1.31±1.40
FTIR 2003–2009	−0.04±0.66	−0.09±1.43
KASIMA	+1.51±0.07	+2.49±0.12
KASIMA summer/autumn	+1.54±0.10	+2.21±0.14
KASIMA summer/autumn on FTIR days	+1.56±0.23	+2.19±0.31
KASIMA on FTIR days	+1.21±0.19	+2.04±0.31
KASIMA 1996–2002	+2.58±0.18	+4.30±0.30
KASIMA 2003–2009	+0.80±0.21	+1.38±0.35

In order to determine the confidence interval for a trend calculated like this, it is necessary to make an assumption on the distribution of the deviations of the data points from the fit. They might not be normally (Gaussian) distributed, for example due to inter-annual variations (resulting e.g. from the changing position and different development of the stratospheric polar vortex) which the function defined by Eq. (1) cannot account for. Therefore, the bootstrap resampling method is applied to estimate the precision of the calculated trends (Efron, 1979; Efron and Tibshirani, 1993). This method has already been used in trend studies from FTIR measurements (Gardiner et al., 2008; Mikuteit, 2008; Vigouroux et al., 2008). It does not make any assumption on the distribution of the differences between data and least linear squares fit. It only assumes that there are enough data points for the deviations to sufficiently represent the underlying distribution themselves. The calculated deviations are added randomly (with replacement) to the best fit in order to create a new artificial data set with the same underlying distribution of the "random" effects. Now the function defined by Eq. (1) is fitted to the artificial data set which results in another value for the trend and the other fitting parameters. This resampling procedure is repeated 5000 times. From the 2.5 and 97.5 percentiles of the 5000 artificial trend values, a mean precision describing the 95 % confidence interval is calculated. This would correspond to about two standard deviations if a normal distribution had been assumed instead.

5 Results and discussion

5.1 HF

As already mentioned, there are no explicit restrictions concerning the emission of fluorine, unlike the case for chlorine and bromine. FTIR measurements from Kitt Peak (Arizona, USA) show a strong increase of the HF column abundance
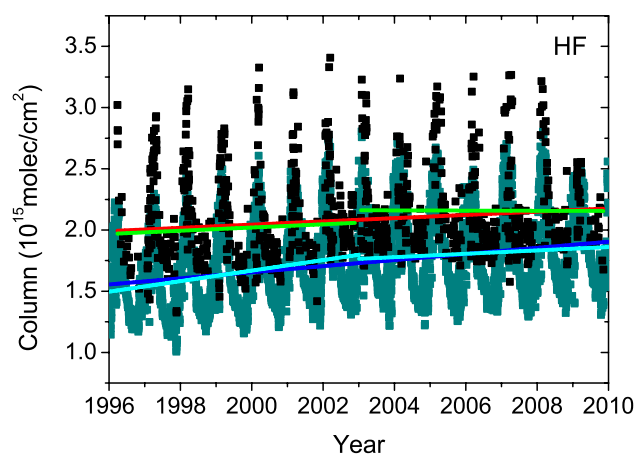
Fig. 2. Time series of FTIR measurements (black squares) and KASIMA model data (dark cyan squares) of HF above Kiruna from March 1996 to November 2009 and January 1996 to December 2009, respectively. The red and dark blue lines represent the linear portion of the least squares fit of Eq. (1) to the measurements and model results, respectively, from 1996 to 2009. The green and cyan lines show the fits to the FTIR and KASIMA data, respectively, from 1996 to 2002 and 2003 to 2009.

with (10.9±1.1) %/yr from 1977 to 1990 (Rinsland et al., 1991) that weakened during the 1990s: The trend from 1977 to 2001 amounts to (4.30±0.15) %/yr (Rinsland et al., 2002).

For the time period investigated here (1996–2009), the trend of the HF column from the FTIR measurements in Kiruna is much weaker, but still positive: (+0.65±0.25) %/yr corresponding to (+1.32±0.50) × 10^{13} molec/(cm² yr) (Fig. 2).

If the time series is cut into two parts, the trend result is about the same from 1996 to 2002, but between 2003 and 2009, no change in the HF vertical column abundance is detectable (Table 1). Still, one should keep in mind that when
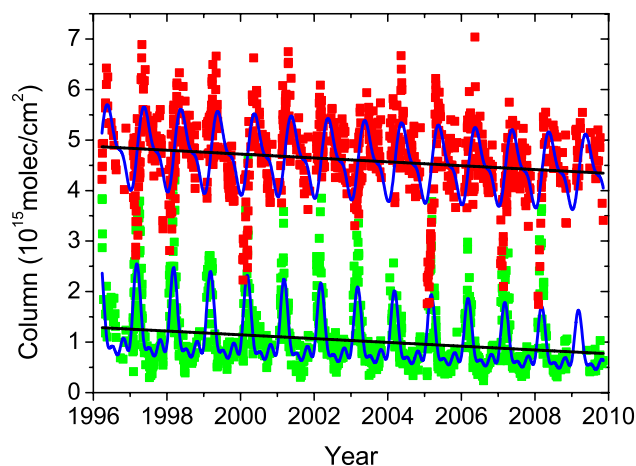
Fig. 3. Time series of HCl (red squares) and ClONO$_2$ (green squares) FTIR measurements in Kiruna from March 1996 until November 2009. The blue lines represent the least squares fit of Eq. (1) to each series, the black lines show the linear part of the fit result only.

the time series are cut, the remaining ones are only 7 years long and thus too short to determine a reliable trend (see also Weatherhead et al., 1998).

The trend modelled by KASIMA for HF above Kiruna over the complete time period amounts to $(+1.51\pm0.07)$ %/yr corresponding to $(+2.49\pm0.12) \times 10^{13}$ molec/(cm^2 yr). So in this case, the model shows a stronger increase than the FTIR instrument observes. Part of the discrepancy can be explained by different sampling (Table 1): The trend from the KASIMA data on days with FTIR measurements only is weaker than that from all KASIMA data. When using only the measurements between June and November ("summer/autumn") and fitting just the linear part of Eq. (1), the FTIR trend is stronger than for all data (Table 1). When the KASIMA results on FTIR days are reduced to the summer/autumn period, a slightly but not significantly larger trend than for all KASIMA data on FTIR days is found. These investigations suggest a strong influence of sampling and the seasonal cycle on the trend calculated from the HF measurements. At the International Scientific Station of the Jungfraujoch, the seasonal cycle of HF measured by the FTIR instrument there was investigated (Duchatelet et al., 2010). Especially the seasonal cycle of the lower stratosphere partial columns and of the total column abundances were found to be anti-correlated with tropopause height, which is due to the high stability of HF. This is why we assume that the main characteristics of the seasonal cycle of the HF total column abundances above Kiruna result both from the varying tropopause height and from the polar vortex.

If the KASIMA HF series is cut into two like the FTIR one, the trend from 1996 to 2002 is stronger than the one for the whole series (Table 1). The trend between 2003 and

2009 is still positive, but relatively weak. So qualitatively, the FTIR measurements and KASIMA model calculations seem to agree on a stabilisation of the atmospheric HF content. Due to the shortness of the time series when they are divided into two parts, these trends should not be trusted quantitatively (see also Weatherhead et al., 1998).

5.2 HCl and ClONO$_2$

According to previous measurements, the total combined abundances of anthropogenic ozone-depleting substances peaked around 1992–1994 in the troposphere and in the mid to late 1990s in the stratosphere (WMO, 2007). Therefore the trends for the total column abundances of HCl and ClONO$_2$ from the FTIR measurements in Kiruna are expected to be negative over the time period considered here (March 1996 to November 2009). This is indeed the case, but the relative trends differ considerably: The resulting value for HCl is (-0.81 ± 0.23) %/yr and for ClONO$_2$ (-3.28 ± 0.56) %/yr (Fig. 3 and Table 2). The absolute trends agree within their error bars: For HCl it amounts to $(-3.83\pm1.10) \times 10^{13}$ molec/(cm^2 yr) and for ClONO$_2$ to $(-3.75\pm0.70) \times 10^{13}$ molec/(cm^2 yr).

The sign and order of magnitude of the result for HCl from the FTIR data is consistent with measurements by the MLS (Microwave Limb Sounder) instrument aboard the Aura satellite. The relative trend determined by Froidevaux et al. (2006) for the layer between 0.7 and 0.1 hPa between 60° N and 60° S for August 2004 through January 2006 amounts to (-0.78 ± 0.08) %/yr.

Compared to the FTIR measurements, both the relative and the absolute trends calculated from the KASIMA model output for about the same time period are weaker (Table 2). The relative trend for HCl from January 1996 to December 2009 is (-0.17 ± 0.06) %/yr and for ClONO$_2$ (-0.90 ± 0.10) %/yr. It is interesting that KASIMA also shows a disparity of about a factor of four between the relative trends of HCl and ClONO$_2$, quite similar to the FTIR data. And like the ones from the measurements, the absolute trends of HCl and ClONO$_2$ from the KASIMA data agree within their errors: The HCl trend amounts to $(-0.67\pm0.25) \times 10^{13}$ molec/(cm^2 yr) and the ClONO$_2$ one to $(-0.84\pm0.10) \times 10^{13}$ molec/(cm^2 yr).

We have not yet found an explanation for the different trends of HCl and ClONO$_2$ above Kiruna. A comparison of FTIR and modelled total column abundances of HCl, ClONO$_2$, and HF and their temporal development at 17 measurement sites around the world belonging to the NDACC is in preparation at the moment (Kohlhepp et al., 2011). At some other northern polar FTIR sites, the signal seems to be similar to the one at Kiruna described here, both for models and measurements. For HCl, FTIR measurements from the midlatitude site on Jungfraujoch show a trend of (-0.87 ± 0.10) %/yr between 1996 and 2009 (Mahieu et al., 2010), which very well matches the HCl trend at Kiruna

Table 2. Absolute and relative trends for HCl and ClONO$_2$ column abundances from the FTIR measurements and KASIMA model calculations for Kiruna. The time range considered is 1996–2009. The "summer/autumn" time series contain the data between June and November only.

species	data source	relative trend (%/yr)	absolute trend (10^{13} molec/(cm^2 yr))
HCl	FTIR	-0.81 ± 0.23	-3.83 ± 1.10
HCl	FTIR summer/autumn	-0.65 ± 0.25	-3.12 ± 1.20
HCl	KASIMA	-0.17 ± 0.06	-0.67 ± 0.25
HCl	KASIMA summer/autumn	-0.26 ± 0.08	-0.97 ± 0.29
HCl	KASIMA summer/autumn on FTIR days	-0.24 ± 0.19	-0.89 ± 0.69
HCl	KASIMA start/end like FTIR	-0.33 ± 0.06	-1.28 ± 0.25
HCl	KASIMA on FTIR days	-0.33 ± 0.17	-1.29 ± 0.65
ClONO$_2$	FTIR	-3.28 ± 0.56	-3.75 ± 0.70
ClONO$_2$	FTIR summer/autumn	-3.25 ± 0.59	-2.60 ± 0.52
ClONO$_2$	KASIMA	-0.90 ± 0.10	-0.84 ± 0.10
ClONO$_2$	KASIMA summer/autumn	-1.06 ± 0.16	-0.74 ± 0.12
ClONO$_2$	KASIMA summer/autumn on FTIR days	-1.49 ± 0.35	-1.00 ± 0.25
ClONO$_2$	KASIMA start/end like FTIR	-1.04 ± 0.11	-0.98 ± 0.10
ClONO$_2$	KASIMA on FTIR days	-1.43 ± 0.28	-1.33 ± 0.28
HCl + ClONO$_2$	FTIR	-1.54 ± 0.23	-9.10 ± 1.42
HCl + ClONO$_2$	FTIR summer/autumn	-1.00 ± 0.25	-5.58 ± 1.44
HCl + ClONO$_2$	KASIMA	-0.31 ± 0.07	-1.51 ± 0.32
HCl + ClONO$_2$	KASIMA summer/autumn	-0.39 ± 0.08	-1.71 ± 0.37

presented above. In contrast, the ClONO$_2$ trend at Jungfraujoch amounts to (-0.90 ± 0.27) %/yr. It is thus much weaker than the one at Kiruna and agrees with the HCl one within errors. Mahieu et al. (2010) also compared their FTIR data with KASIMA model results when sampled like the measurements. KASIMA simulates a relative ClONO$_2$ decrease of (-0.72 ± 0.21) %/yr for Jungfraujoch that is about a factor of two stronger than the HCl one of (-0.29 ± 0.11) %/yr.

Part of the disparity between modelled and measured trends can be explained by the slightly different start and end dates combined with the annual cycle of the considered species: When the KASIMA time series of HCl and ClONO$_2$ are started and ended exactly on the same days as the FTIR series in March 1996 and November 2009, respectively, the trends become stronger and thus slightly closer to the FTIR results (Table 2). To investigate the influence of sampling on the differences between model and measurements, the KASIMA results were restricted to the days with FTIR measurements. Concerning the HCl time series, sampling does not seem to have a strong influence. For ClONO$_2$, the KASIMA trend on FTIR days only is stronger than the one with the FTIR start and end days and thus even closer to the trend from the FTIR measurements (Table 2).

When the linear part of Eq. (1) is fitted to the data between June and November ("summer/autumn"), the HCl and ClONO$_2$ trends from KASIMA are larger and those from FTIR smaller than for the respective whole time series so that the trends from model and measurements become more alike (Table 2). The trend of ClONO$_2$ from the KASIMA

data on FTIR days in summer/autumn is even closer to the FTIR summer/autumn results, while for HCl, the sampling influence is negligible again. Still, as the error bars are larger for the KASIMA data on FTIR days in summer/autumn, they overlap with the ones of nearly all other trend results.

The difference between the trend from all data and the one from the summer/autumn data only is likely partly due to the fact that the linear least squares fit is not able to completely capture the large column abundances especially of ClONO$_2$ in spring. This particularly concerns the FTIR data as the annual cycle is more pronounced in the measurements than in the model results.

It is already known (Hamann, 2007; Mikuteit, 2008) and can also be seen in Fig. 4 that KASIMA tends to underestimate the measured HCl total column abundances by about 20 %. One reason for this is that KASIMA does not include the part of the troposphere below 7 km. Instead, a lower boundary condition has to be prescribed. This of course influences the total column abundances. Furthermore, some tropospheric processes, for example, wash-out, have to be parameterised because the model does not simulate cloud or rain droplets. Depending on the data set used for nudging in KASIMA, the atmospheric dynamics varies. This can cause changes in the resulting total column abundances, too (Hamann, 2007). Increasing the horizontal resolution (to T42 instead of T21 which was used here) also leads to more realistic HCl column abundances because the processes at the polar vortex edge are represented more precisely (Hamann, 2007).
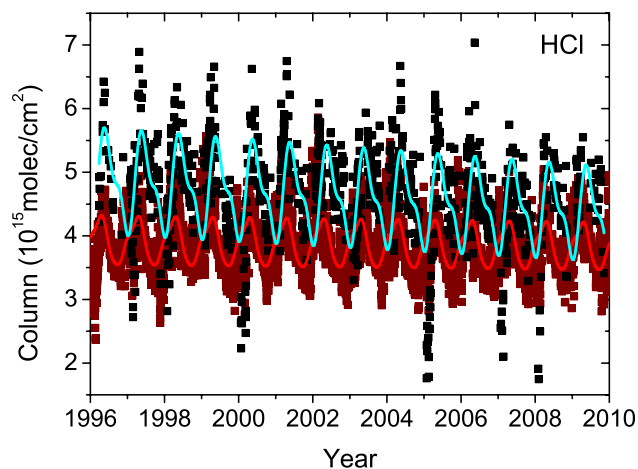
Fig. 4. Time series of FTIR measurements (black squares) and KASIMA model data (dark red squares) of HCl above Kiruna from 1996 to 2009 and the least squares fits of Eq. (1) to the measurements (cyan line) and model data (red line).
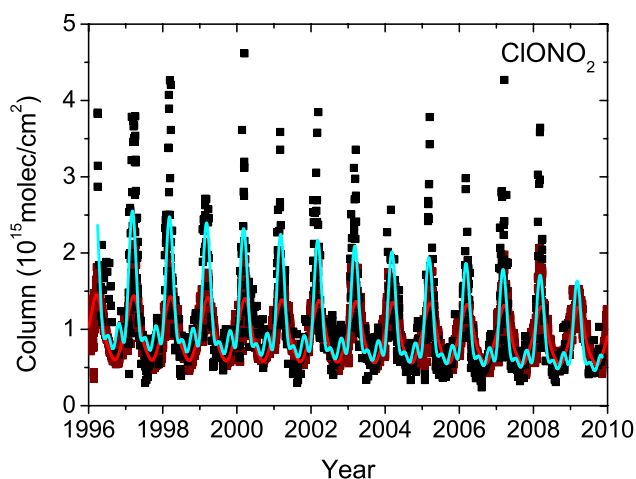

Fig. 5. Time series of FTIR measurements (black squares) and KASIMA model data (dark red squares) of ClONO$_2$ above Kiruna from 1996 to 2009 and the least squares fits of Eq. (1) to the measurements (cyan line) and model data (red line).

In case of ClONO$_2$, KASIMA agrees very well with the FTIR measurements (Fig. 5). Only the maxima at the late vortex edge are underestimated by the model due to its limited horizontal resolution. One reason for the good agreement might be that the tropospheric ClONO$_2$ partial column is negligible and the argument concerning the prescribed tropospheric partial columns in KASIMA does not apply strongly to ClONO$_2$.

The trend of the sum of the HCl and ClONO$_2$ column abundances amounts to (-1.54 ± 0.23) %/yr corresponding to $(-9.10\pm1.42) \times 10^{13}$ molec/(cm^2 yr) for the FTIR measurements and (-0.31 ± 0.07) %/yr corresponding

to $(-1.51\pm0.32) \times 10^{13}$ molec/(cm^2 yr) for the KASIMA data. The model value reflects the CFC and HCFC content prescribed according to the WMO (2007) Ab scenario. As seen already in the separate trends for HCl and ClONO$_2$, there is a large difference between the modelled and measured trends which can partly be explained by the different start and end days and sampling. When using the summer/autumn data only and fitting a linear trend, the KASIMA and FTIR results become more similar (Table 2).

6 Conclusions

The trend of HF is expected to be positive for the time range between 1996 and 2009. This is indeed the case for both the measurements and model calculations investigated here. The time series from the FTIR spectrometer shows an increase of the HF total column abundances by $(+0.65\pm0.25)$ %/yr which is weaker than the $(+1.51\pm0.07)$ %/yr trend simulated by KASIMA.

When the FTIR time series of HF is divided into two parts, the calculated trends are not significant. One reason for this is that the two parts are simply too short to detect a reliable trend (see also Weatherhead et al., 1998). Still, the trend result is much smaller for the second half than for the first half both for the FTIR measurements and the KASIMA simulations. This suggests a decrease of the positive trend or even a stabilisation of the HF column abundance in the last few years.

Both FTIR measurements and KASIMA model calculations show a significant decrease of the HCl and ClONO$_2$ vertical column abundances above Kiruna. The relative trends from KASIMA are (-0.17 ± 0.06) %/yr and (-0.90 ± 0.10) %/yr for HCl and ClONO$_2$, respectively. They are thus weaker than those calculated from the measurements which amount to (-0.81 ± 0.23) %/yr and (-3.28 ± 0.56) %/yr for HCl and ClONO$_2$, respectively. There is a factor of about four between the relative trends of HCl and ClONO$_2$ in both measurement and model data. This can be seen in other northern polar FTIR and model data as well (Kohlhepp et al., 2011). The reason for this difference is currently under investigation.

It has been shown that the start and end date and also sampling influence the resulting trend. For the model time series sampled like the FTIR measurements, the trends are stronger than when using all KASIMA data and thus more similar to those from the measurements.

The trends of HCl, ClONO$_2$, and of their sum from model and measurements are also closer to each other when only the summer/autumn data between June and November are used. One can conclude that the strong annual cycle largely due to the processes in the polar vortex can influence the trend results.

References

Barret, B., Hurtmans, D., Carleer, M. R., de Mazière, M., Mahieu, E., and Coheur, P.-F.: Line narrowing effect on the retrieval of HF and HCl vertical profiles from ground-based FTIR measurements, J. Quant. Spectrosc. Radiat. Transfer, 95, 499–519, 2005.

Bian, H. and Prather, M. J.: Fast-J2: Accurate simulation of stratospheric photolysis in global chemical models, J. Atmos. Chem., 41, 281–296, 2002.

Chipperfield, M. P., Burton, M., Bell, W., Paton-Walsh, C., Blumenstock, T., Coffey, M. T., Hannigan, J. W., Mankin, W. G., Galle, B., Mellqvist, J., Mahieu, E., Zander, R., Notholt, J., Sen, B., and Toon, G. C.: On the use of HF as a reference for the comparison of stratospheric observations and models, J. Geophys. Res., 102, 12901–12919, 1997.

Duchatelet, P., Demoulin, P., Hase, F., Ruhnke, R., Feng, W., Chipperfield, M. P., Bernath, P. F., Boone, C. D., Walker, K. A., and Mahieu, E.: Hydrogen fluoride total and partial column time series above the Jungfraujoch from long-term FTIR measurements: Impact of the line-shape model, characterization of the error budget and seasonal cycle, and comparison with satellite and model data, J. Geophys. Res., 115, D22306, doi:10.1029/2010JD014677, 2010.

Efron, B.: Bootstrap Methods: Another look at the Jackknife, The Annals of Statistics, 7(1), 1–26, 1979.

Efron, B. and Tibshirani, R.: An Introduction to the Bootstrap, Mg. Stat. Pro., 57, 456 pp., 1993.

Froidevaux, L., Livesey, N. J., Read, W. G., Salawitch, R. J., Waters, J. W., Drouin, B., MacKenzie, I. A., Pumphrey, H. C., Bernath, P., Boone, C., Nassar, R., Montzka, S., Elkins, J., Cunnold, D., and Waugh, D.: Temporal decrease in upper atmospheric chlorine, Geophys. Res. Lett., 33, L23812, doi:10.1029/2006GL027600, 2006.

Gardiner, T., Forbes, A., de Maziére, M., Vigouroux, C., Mahieu, E., Demoulin, P., Velazco, V., Notholt, J., Blumenstock, T., Hase, F., Kramer, I., Sussmann, R., Stremme, W., Mellqvist, J., Strandberg, A., Ellingsen, K., and Gauss, M.: Trend analysis of greenhouse gases over Europe measured by a network of ground-based remote FTIR instruments, Atmos. Chem. Phys., 8, 6719–6727, doi:10.5194/acp-8-6719-2008, 2008.

Hamann, K.: Untersuchung des Trends halogenhaltiger Verbindungen in der Stratosphäre, Diploma thesis at the Institute for Meteorology and Climate Research (IMK-ASF), University of Karlsruhe, 2007.

Hase, F.: Inversion von Spurengasprofilen aus hochaufgelösten bodengebundenen FTIR-Messungen in Absorption, Wissenschaftliche Berichte, FZKA-Report No. 6512, Forschungszentrum Karlsruhe, Germany, 2000.

Hase, F., Blumenstock, T., and Paton-Walsh, C.: Analysis of the instrumental line shape of high-resolution Fourier transform IR spectrometers with gas cell measurements and new retrieval software, Appl. Optics, 38, 3417–3422, 1999.

Hase, F., Hannigan, J. W., Coffey, M. T., Goldman, A., Höpfner, M., Jones, N. B., Rinsland, C. P., and Wood, S. W.: Intercomparison of retrieval codes used for the analysis of high-resolution, ground-based FTIR measurements, J. Quant. Spectrosc. Radiat. Transfer, 87, 25–52, 2004.

Kohlhepp, R., Ruhnke, R., Chipperfield, M. P., de Mazière, M., Notholt, J., Barthlott, S., Batchelor, R. L., Blatherwick, R. D., Blumenstock, T., Coffey, M. T., Duchatelet, P., Fast, H., Feng, W., Goldman, A., Griffith, D. W. T., Hamann, K., Hannigan, J. W., Hase, F., Jones, N. B., Kagawa, A., Kaiser, I., Kasai, Y., Kirner, O., Kouker, W., Lindenmaier, R., Mahieu, E., Mittermeier, R. L., Monge-Sanz, B., Murata, I., Nakajima, H., Morino, I., Palm, M., Paton-Walsh, C., Reddmann, T., Rettinger, M., Rinsland, C. P., Rozanov, E., Schneider, M., Senten, C., Sinnhuber, B.-M., Smale, D., Strong, K., Sussmann, R., Taylor, J. R., Vanhaelewyn, G., Warneke, T., Whaley, C., Wiehle, M., and Wood, S. W.: Observed and simulated time evolution of HCl, ClONO$_2$, and HF total columns, Atmos. Chem. Phys. Discuss., in preparation, 2011.

Kouker, W., Langbein, I., Reddmann, T., and Ruhnke, R.: The Karlsruhe Simulation Model of the Middle Atmosphere (KASIMA), Wissenschaftliche Berichte, FZKA-Report No. 6278, Forschungszentrum Karlsruhe, Germany, 1999.

Mahieu, E., Rinsland, C. P., Gardiner, T., Zander, R., Demoulin, P., Chipperfield, M. P., Ruhnke, R., Chiou, L. S., de Mazière, M., Duchatelet, P., Lejeune, B., Roland, G., and Servais, C.: Recent trends of inorganic chlorine and halogenated source gases above the Jungfraujoch and Kitt Peak stations derived from high-resolution FTIR solar observations, EGU General Assembly 2010, held 2–7 May, 2010 in Vienna, Austria, p. 2420, 2010.

Mikuteit, S.: Trendbestimmung stratosphärischer Spurengase mit Hilfe bodengebundener FTIR-Messungen, Wissenschaftliche Berichte, FZKA-Report No. 7385, Forschungszentrum Karlsruhe, Germany, 2008.

Molina, M. J. and Rowland, F. S.: Stratospheric sink for chlorofluoromethanes: chlorine atom – catalysed destruction of ozone, Nature, 249, 810–812, 1974.

Reddmann, T., Ruhnke, R., and Kouker, W.: Three-dimensional model simulations of SF$_6$ with mesospheric chemistry, J. Geophys. Res., 106, 14525–14537, 2001.

Rinsland, C. P., Levine, J. S., Goldman, A., Sze, N. D., Ko, M. K. W., and Johnson, D. W.: Infrared measurements of HF and HCl total column abundances above Kitt Peak, 1997–1990: Seasonal cycles, long-term increases, and comparisons with model calculations, J. Geophys. Res., 96, 15523–15540, 1991.

Rinsland, C. P., Zander, R., Mahieu, E., Chiou, L. S., Goldman, A., and Jones, N. B.: Stratospheric HF column abundances above

Kitt Peak (31.9° N latitude): trends from 1977 to 2001 and correlations with stratospheric HCl columns, J. Quant. Spectrosc. Radiat. Transfer, 74, 205–216, 2002.

Rodgers, C. D.: Inverse Methods for Atmospheric Sounding: Theory and Praxis, World Scientific Publishing Co., Singapore, 2000.

Rothman, L. S., Jacquemart, D., Barbe, A., Benner, D. C., Birk, M., Brown, L. R., Carleer, M. R., Chackerian, C. J., Chance, K., Coudert, L. H., Dana, V., Devi, V. M., Flaud, J.-M., Gamache, R. R., Goldman, A., Hartmann, J.-M., Jucks, K. W., Maki, A. G., Mandin, J.-Y., Massie, S. T., Orphal, J., Perrin, A., Rinsland, C. P., Smith, M. A. H., Tennyson, J., Tolchenov, R. N., Toth, R. A., Auwera, J. V., Varanasi, P., and Wagner, G.: The HITRAN 2004 molecular spectroscopic database, J. Quant. Spectrosc. Radiat. Transfer, 96, 139–204, 2005.

Ruhnke, R., Kouker, W., and Reddmann, T.: The influence of the OH + NO$_2$ + M reaction on the NOy partitioning in the late Arctic winter 1992/1993 as studied with KASIMA, J. Geophys. Res., 104, 3755–3772, 1999.

Stiller, G. P., von Clarmann, T., Höpfner, M., Glatthor, N., Grabowski, U., Kellmann, S., Kleinert, A., Linden, A., Milz, M., Reddmann, T., Steck, T., Fischer, H., Funke, B., López-Puertas, M., and Engel, A.: Global distribution of mean age of stratospheric air from MIPAS SF$_6$ measurements, Atmos. Chem. Phys., 8, 677–695, doi:10.5194/acp-8-677-2008, 2008.

Vigouroux, C., De Maziére, M., Demoulin, P., Servais, C., Hase, F., Blumenstock, T., Kramer, I., Schneider, M., Mellqvist, J., Strandberg, A., Velazco, V., Notholt, J., Sussmann, R., Stremme, W., Rockmann, A., Gardiner, T., Coleman, M., and Woods, P.: Evaluation of tropospheric and stratospheric ozone trends over Western Europe from ground-based FTIR network observations, Atmos. Chem. Phys., 8, 6865–6886, doi:10.5194/acp-8-6865-2008, 2008.

Wagner, G. and Birk, M.: New infrared spectroscopic database for chlorine nitrate, J. Quant. Spectrosc. Radiat. Transfer, 82, 443–460, 2003.

Weatherhead, E. C., Reinsel, G. C., Tiao, G. C., Meng, X.-L., Choi, D., Cheang, W.-K., Keller, T., DeLuisi, J., Wuebbles, D. J., Kerr, J. B., Miller, A. J., Oltmans, S. J., and Frederick, J. E.: Factors affecting the detection of trends: Statistical considerations and applications to environmental data, J. Geophys. Res., 103, 17149–17161, 1998.

WMO: Scientific assessment of ozone depletion: 2002, Global ozone research and monitoring project – report no. 47, Geneva, Switzerland, 2003.

WMO: Scientific assessment of ozone depletion: 2006, Global ozone research and monitoring project – report no. 50, Geneva, Switzerland, 2007.

Zander, R., Mahieu, E., Demoulin, P., Duchatelet, P., Roland, G., Servais, C., De Mazière, M., Reimann, S., and Rinsland, C. P.: Our changing atmosphere: Evidence based on long-term infrared solar observations at the Jungfraujoch since 1950, Sci. Total Environ., 391, 184–195, 2008.